https://doi.org/10.5194/egusphere-2026-4656
Preprint. Discussion started: 7 September 2026

An integrated framework for wildfire risk assessment under climate change: empirical validation and application in Greece

Anna Karali [1,2,4], Maria Hatzaki[2], Konstantinos V. Varotsos[1], Aristea Koliou[3], Nikolaos Fyllas[3,4], Varvara Antoniou[5], Christos Giannakopoulos[1]

[1]Institute for Environmental Research and Sustainable Development, National Observatory of Athens, Lofos Koufou, 15236 Palaia Penteli, Athens, Greece
[2] Section of Geography and Climatology, Department of Geology and Environment, National and Kapodistrian University of Athens, University Campus, 15784 Zografou, Athens, Greece
[3]Section of Ecology and Taxonomy, Department of Biology, National and Kapodistrian University of Athens, Athens, University Campus, 15784 Zografou, Athens, Greece
[4]Biodiversity Conservation Laboratory, Department of Environment, University of the Aegean, University Hill, 81100 Mytilene, Greece
[5]School of Rural, Surveying and Geoinformatics Engineering, National Technical University of Athens, University Campus, 15780 Zografou Athens, Greece

Correspondence to: Anna Karali (akarali@noa.gr)

Abstract. Climate change is increasing the frequency and severity of wildfires across the Mediterranean, posing growing risks to ecosystems, infrastructure and human communities. Robust methodologies for assessing wildfire risk under both present and future climate conditions are therefore essential to support climate change adaptation. In this study, we develop and empirically validate an integrated wildfire risk assessment framework for Greece following the Intergovernmental Panel on Climate Change risk concept. Wildfire hazard, exposure and vulnerability are represented through climate, environmental and socioeconomic indicators, while alternative hazard representations and aggregation approaches were systematically evaluated against observed wildfire occurrence to identify the most accurate methodological configuration. The validated framework was then applied to assess wildfire risk for the reference period (1995–2014) and under SSP2-4.5 and SSP5-8.5 scenarios for the near (2041–2060) and distant (2081–2100) future. The results demonstrated that aggregation behaviour plays a critical role in determining the predictive performance of composite wildfire risk indices, with an Ordered Weighted Averaging (OWA) approach providing a statistically significant improvement over conventional linear aggregation. Analysis of component contributions identified hazard as the dominant contributor to wildfire risk across most municipalities, although exposure and vulnerability remained important determinants of the final risk patterns. Future projections indicated a widespread increase in wildfire risk throughout Greece, with the largest increases occurring under the high-end SSP5-8.5 scenario in the late century. The proposed framework provides a transparent and empirically validated basis for wildfire risk assessment that can support climate change adaptation planning at national and regional scales.

https://doi.org/10.5194/egusphere-2026-4656
Preprint. Discussion started: 7 September 2026

1 Introduction

Under changing climatic conditions, both fire danger and the frequency and extent of wildfires are expected to increase across the Mediterranean basin (Carnicer et al., 2022, Rovithakis et al., 2022, Dupuy et al., 2020; Ruffault et al., 2020; Turco et al., 2018). Recent projections suggest that southern Europe could experience up to a tenfold increase in the probability of catastrophic wildfires by the end of the century, even under moderate climate change scenarios (El Garroussi et al., 2024). Additionally, according to Grünig et al. (2023), the Mediterranean fire regimes are highly sensitive to changes in future climate, with the probability of extremely large fires more than doubling by the end of the century. Based on the findings of the first European Climate Risk Assessment (EUCRA), a seminal report intended to inform climate policy in Europe, wildfire-related risks are already rated as critical in southern Europe and are expected to become catastrophic for biodiversity and carbon sinks by the end of the century under high-emission scenarios. Together, these findings underscore the need for improved wildfire risk assessment and climate change adaptation strategies at both European and national scales.

Consistent with the projections for the Mediterranean Basin, Greece is expected to face a warmer and drier future. Under the high-emission scenario (RCP8.5), annual mean temperatures are projected to increase by up to 4.3°C across the country by 2100, while annual precipitation is projected to decrease by 16% (Georgoulias et al., 2022). According to Rovithakis et al. (2022), under the same emission scenario, high fire danger days will increase throughout Greece with the eastern and northern part of the country encountering increases by up to 40 additional days per year by the late 21st century.

Greece has already experienced a significant increase in wildfire frequency, severity, and extent, a trend driven by climatic, socio-economic factors and land-use changes, including rural depopulation and land abandonment and the unregulated expansion of the wildland-urban interface (WUI) (OECD, 2023). Further underpinning this, the recent report on wildfires of the Organisation for Economic Co-operation and Development (OECD) for Greece, emphasizes that extreme forest and peri-urban wildfires during the last two decades, such as those recorded in 2007 (Peloponnese), 2018 (Mati - Attica) and 2023 (Evros and Attica region), have repeatedly exceeded national suppression capacity, leading to severe environmental degradation, economic damage and losses of human lives (OECD, 2024).

As suppression alone struggles to limit the growing impacts of extreme fire events, climate change adaptation should be a central tenet of wildfire policy (OECD, 2023). In accordance with international shift on focus, the Greek National Forest Strategy (2018–2038) explicitly acknowledges the impacts of climate change on forests and prioritizes climate adaptation in the management of both forests and WUI areas (Ministry of Environment and Energy, 2018).

Comprehensive wildfire risk assessments are a fundamental step in wildfire management, as they provide the information base for all prevention and adaptation policies and measures (OECD, 2023). A widely adopted approach for assessing climate-related risk was introduced in the Fifth Assessment Report (AR5) of the Intergovernmental Panel on Climate Change (IPCC), which defines risk as the potential for adverse consequences arising from the interaction of hazard, exposure and vulnerability (IPCC, 2014). This framework is retained in the Sixth Assessment Report (AR6), which further emphasizes the dynamic interactions among these components under climate change (IPCC, 2022). Within this framework, hazard refers to

https://doi.org/10.5194/egusphere-2026-4656
Preprint. Discussion started: 7 September 2026

the potential occurrence of climate-related physical events or trends, exposure describes the presence of people, ecosystems and assets that could be adversely affected, while vulnerability reflects their propensity to experience harm, including both sensitivity and adaptive capacity.

Given that climate change-informed wildfire risk assessment remains underdeveloped in Greece (OECD, 2024), this study develops and empirically evaluates a methodological framework for quantifying wildfire risk under both present and future climatic conditions. Consistent with the IPCC risk concept, the proposed methodology integrates hazard, exposure and vulnerability into a composite risk index at the municipal scale. Indicator weights are derived using the Analytic Hierarchy Process (AHP), while alternative hazard representations and aggregation frameworks are systematically evaluated against historical wildfire occurrence to identify the methodological configuration with the highest predictive performance. The resulting composite risk index characterizes the spatial distribution of wildfire risk conditions across municipalities and is subsequently applied under multiple climate change scenarios to assess future changes in wildfire risk. The following sections describe the proposed framework, evaluate alternative hazard representations and aggregation frameworks, and demonstrate its application for present and future wildfire risk assessment in Greece.

2 Methods and Data

2.1 Climatic and fire data

2.1.1 CMIP6 Global Climate Models (GCMs)

To calculate the hazard component of wildfire risk, daily climatic outputs from three CMIP6 Global Climate Models (GCMs), available through the Copernicus Climate Change Service (C3S) Climate Data Store (CDS), were used. The GCM sub-ensemble comprised the EC-Earth3-Veg (Döscher et al., 2022), MPI-ESM1-2-HR (Müller et al., 2018) and MIROC6 (Tatebe et al., 2019) models.

2.1.2 ERA5-Land reanalysis dataset

The ERA5-Land reanalysis dataset (Muñoz-Sabater, 2019), available through the Copernicus Climate Change Service (C3S) Climate Data Store (CDS), was used as the reference observational dataset for the statistical downscaling of climate projections. ERA5-Land provides hourly estimates of land-surface variables at a spatial resolution of approximately 9 km from 1950 onwards (Muñoz-Sabater et al., 2021). Daily maximum temperature, minimum relative humidity, mean wind speed and total daily precipitation were extracted from ERA5-Land for the calculation of hazard indicators.

2.1.3 Fire statistics

Fire occurrence data were obtained from the Hellenic Fire Service for the 2000-2014 period. The original dataset reported, among other information, the location name (without geographic coordinates) where the fire occurred, the date and time of

https://doi.org/10.5194/egusphere-2026-4656
Preprint. Discussion started: 7 September 2026

fire ignition, and the area burned by land use type (including forests, forested areas, agricultural lands etc.). The location name was used to identify the coordinates of each event. We cross-checked the location identification by visually inspecting changes in Google Earth imagery for images taken before and after the reported wildfire date. Additionally, we cross-checked wildfire location by inspecting whether it was identified in the Burn Scar Mapping (BSM) data portal (http://ocean.space.noa.gr/diachronic_bsm/). An event was given a geolocation and maintained in the dataset only if it was identified in either one of the satellite data sources.

2.2 IPCC risk framework and indicators selection

The selection of indicators for the assessment of wildfire risk was based on a comprehensive approach combining literature review and stakeholder consultation. Key references included climate-related fire risk studies (Bacciu et al., 2021; Chuvieco et al., 2023; El Mazi et al., 2024; Khan et al., 2026; Lamat et al., 2021; Nuthammachot and Stratoulias, 2021; Papanikolaou et al., 2012; Marquez Torez et al., 2023) and European strategic reports and risk assessment frameworks (Oom et al., 2022; Eklund et al., 2023). Indicators were chosen to comprehensively address the three IPCC risk components (hazard, exposure and vulnerability) taking into consideration data availability. Stakeholders involved in our study further validated the relevance and importance of the selected indicators, integrating both scientific and practical perspectives.

2.2.1 Hazard component

The climatic hazard component was assessed using indicators derived from the Canadian Fire Weather Index (FWI) System. Developed as part of the Canadian Forest Fire Danger Rating System (CFFDRS), the FWI System has been operationally adopted across Europe through the European Forest Fire Information System (EFFIS) since 2007. It is a meteorologically based fire danger rating system that combines weather variables to estimate fuel moisture conditions, potential fire behaviour and overall fire danger (van Wagner, 1987; Stocks et al., 1989).

To investigate the influence of hazard representation on wildfire risk assessment, three alternative hazard indicators derived from the CFFDRS were evaluated: the Fine Fuel Moisture Code (FFMC), the Initial Spread Index (ISI) and the Fire Weather Index (FWI). These indices represent complementary aspects of wildfire danger. FFMC primarily reflects the moisture content of fine fuels and their susceptibility to ignition, ISI characterizes the potential rate of fire spread, while FWI provides an integrated measure of overall fire danger by combining fuel moisture and expected fire behaviour (van Wagner, 1987; Wotton, 2009).

For each indicator, the 90th percentile was calculated for the reference period (1995–2014) and for two future periods (2041–2060 and 2081–2100) under the SSP2-4.5 and SSP5-8.5 climate scenarios. The use of the 90th percentile was motivated by its widespread application as a robust indicator of extreme fire-weather conditions in the Mediterranean region, particularly for FWI (e.g., Bedia et al., 2014), and by its previous application and validation in Greece (Varela et al., 2018).

https://doi.org/10.5194/egusphere-2026-4656
Preprint. Discussion started: 7 September 2026

Although percentile-based thresholds are most commonly applied to FWI, the same approach was consistently adopted for FFMC and ISI to enable a comparable representation of extreme fire-weather conditions across the three hazard indicators. Daily fire weather indices were initially calculated separately for each GCM using daily mean temperature, minimum relative humidity, mean wind speed and total daily precipitation. The resulting daily FFMC, ISI and FWI fields were subsequently statistically downscaled following the methodology of Varotsos et al. (2023) and Karali et al. (2023), using ERA5-Land as the reference dataset. For each GCM, the 90th percentile (FFMC90, ISI90, FWI90) was calculated for the baseline and future periods, and the ensemble mean of the three GCMs was subsequently used as the climatic hazard input for the wildfire risk assessment.

2.2.2 Exposure component

In line with the IPCC risk framework (IPCC, 2014), exposure was quantified using indicators representing the spatial distribution of forest areas, agricultural areas, protected areas, and the Wildland–Urban Interface (WUI), thereby capturing the distribution of natural and socio-environmental assets potentially exposed to wildfire hazard (Table 1).

Forest and agricultural areas

Forest and agricultural areas were derived from the Corine Land Cover (CLC) 2018 of the Copernicus Land Monitoring Service (Copernicus Land Monitoring Service, 2020) considering the third level of classification. Forest areas correspond to the following class codes: 311, 312, 313, 321, 322, 323, 324, while the agricultural areas correspond to 211, 221, 222, 223, 224, 231, 243, 244 classes.

Protected areas

Protected areas were derived from the World Database on Protected Areas (WDPA), the most comprehensive global database on terrestrial and marine protected areas (UNEP-WCMC and IUCN, 2025). In the framework of this study, only the polygons representing the terrestrial protected areas of Greece were extracted and used for further analysis.

Wildland-Urban Interface (WUI)

The Wildland-Urban Interface indicator was derived using the global WUI map developed by Schug et al. (2023). The dataset distinguishes eight WUI classes. In this study, only classes 1–4 (intermix and interface WUI) were considered, irrespective of the dominant vegetation type, to represent the presence of WUI at the pixel level.

Table 1: Hazard and exposure indicators together with their native resolution and data source.

Risk component	Index	Description	Resolution	Data source
Hazard	FWI/FFMC/ISI	90^{th} percentile of the index	9km	ERA5-Land (Muñoz-Sabater, 2019); CMIP6 sub-ensemble (Copernicus Climate

https://doi.org/10.5194/egusphere-2026-4656
Preprint. Discussion started: 7 September 2026

				Change Service, 2021)
Exposure	Forests	Binary presence of forests/forested areas at pixel level	100m	CLC 2018 (Copernicus Land Monitoring Service, 2018)
	Agricultural land	Binary presence of agricultural areas at pixel level	100m	CLC 2018 (Copernicus Land Monitoring Service, 2018)
	Protected areas	Binary presence of protected areas at pixel level	-	World Database on Protected Areas WDPA (UNEP-WCMC & IUCN, 2025)
	WUI	Binary presence of WUI at pixel level	10m	Schug et al. (2023)

2.2.3 Vulnerability component: Sensitivity

Sensitivity subcomponent was assessed utilizing a set of biophysical indicators representing key environmental characteristics that influence wildfire susceptibility and behavior, namely flammability, fuel load, slope, aspect and proximity to power transmission networks (Table 2).

Fuel flammability

Fuel flammability was used as a proxy for the inherent propensity of vegetation types to ignite, sustain combustion and contribute to fire spread, reflecting intrinsic structural fuel characteristics rather than the fuel moisture conditions represented by the fire weather indices. In our study, flammability information was adopted from the study of Bacciu et al. (2021), where a flammability index ranging from 1 (very low) to 5 (very high) was assigned to each CLC 2018 land cover type categories based on the methodology of Xanthopoulos et al. (2012) and Corona et al. (2014). Xanthopoulos et al. (2012) developed a flammability classification for 60 forest, shrubland, and grassland types in Europe and North Africa, which was subsequently linked to the corresponding CLC 2018 classes by Bacciu et al. (2021).

Above ground biomass

To quantify above ground biomass available for combustion, two datasets describing live and dead fuels were used. The first dataset is the global dataset of forest above-ground biomass (v5.01) developed by ESA Biomass Climate Change Initiative (Santoro and Cartus, 2024). The dataset is based on Earth observation data from the Copernicus programme and other global remote sensing sources at 100m horizontal resolution. It comprises of estimates of forest above-ground biomass, which is defined as the mass, expressed as oven-dry weight of the woody parts (stem, bark, branches and twigs) of all living trees, excluding stump and roots, for eight years between 2010 and 2021. In our study, the year 2010 was selected for further analysis as was the only available for the period corresponding to current climatic conditions (i.e., 1995–2014). The second dataset is the ECMWF Fuel Characteristics V2 global dataset (McNorton & Di Giuseppe, 2024) which involves above ground fuel load and moisture content data. The dataset combines satellite observations and numerical weather prediction

https://doi.org/10.5194/egusphere-2026-4656
Preprint. Discussion started: 7 September 2026

simulations and is available at a daily temporal step at 9 km spatial horizontal resolution. Daily data of dead (wood and foliage) biomass were averaged for the years 2003-2014 in order to obtain an average status of dead fuel load for the current climatic conditions per pixel. The final total above ground biomass was then calculated at pixel level by summing live and dead fuel data from the abovementioned datasets.

Aspect and slope

Slope and aspect influence fire behavior as well as the area's wildfire sensitivity because of their influence on both vegetation flammability and fire spread. Aspect determines the amount of solar radiation a surface receives, which in turn affects fuel moisture conditions. Faster drying vegetation and increased flammability is a common occurrence for south-facing slopes in the Mediterranean (Mouillot et al., 2003; Oliveira et al., 2014; Robinne et al., 2018). Regarding slope, fires tend to spread faster uphill due to the preheating of fuels ahead of the flame front (Rothermel, 1972). Steeper slopes further enhance surface water runoff, reducing soil moisture retention thus making vegetation more prone to ignition (Sun et al., 2023). Both aspect and slope indices were calculated in ArcGIS Pro utilizing the Copernicus Digital Elevation Model (DEM) GLO-90 (European Space Agency, 2021). After their calculation, aspect and slope data were classified into 5 classes based on the classification system proposed in the framework of LIFE Forest Cities (Local Authorities for Forest Fire Prevention) project, focusing on assessing fire risk and developing fire prevention action plans for selected municipalities in Greece (Papanikolaou et al., 2012).

Power transmission networks

An additional sensitivity indicator considered in this study relates to the distance from medium and high voltage power transmission networks (>45 kV). Sensitivity zones were defined based on the distance from power transmission networks and elevation, according to the technical specifications for the fire protection planning studies issued by the Hellenic Ministry of Environment and Energy. Power line data for Greece were acquired from the OpenStreetMap (OSM) spatial dataset (OpenStreetMap contributors, 2025) and were combined with elevation data (Copernicus DEM). In ArcGIS Pro, a 150-meter buffer was created for the transmission network, and altitudinal classes (0–600 m, 600–1200 m, and >1200 m) were assigned according to the Ministry's specifications. The final sensitivity index was calculated at the pixel level, integrating both proximity and elevation information.

2.2.4 Vulnerability component: Adaptive Capacity

Adaptive capacity was assessed following the vulnerability framework proposed by Eklund et al. (2023), which adopts an indicator-based approach applicable across multiple natural hazards. Based on this framework, firefighter availability, regional Gross Domestic Product (GDP), educational level and employment in the primary sector were selected as proxy indicators of adaptive capacity, considering both data availability and their relevance to wildfire preparedness, response and long-term landscape management (Table 2).

https://doi.org/10.5194/egusphere-2026-4656
Preprint. Discussion started: 7 September 2026

Firefighters and volunteers

The density of firefighters and volunteers (expressed as number per km^2) reflects the regional availability of human resources to respond rapidly and effectively to fire events, thereby reducing potential damages and enhancing overall resilience. Data for the calculation of the indicator were obtained directly from the Hellenic Fire Service, through personal communication, and refer to the operational year 2023.

Occupation in the primary sector

The occupation rate in the primary sector (measured as the number of people employed per km^2) was used as an additional sensitivity indicator. This indicator captures the link between socio-economic trends and fire vulnerability in rural and peri-urban areas. A lower density of workers in the primary sector is associated with the progressive abandonment of rural areas which in turn leads to increased fuel accumulation. Moreover, the decline of agricultural and grazing activities in rural and peri-urban areas, results in the loss of natural fuel breaks that can act as barriers to fire spread (Vilar et al., 2016; Colantoni et al., 2020). To quantify this indicator, the number of people working in the primary sector per regional unit was obtained from the Hellenic Statistical Authority (ELSTAT) (ELSTAT, 2020).

Educational level

Educational level was represented by the proportion of the population with tertiary education, following the indicator-based vulnerability framework of Eklund et al. (2023). Higher educational attainment is associated with greater knowledge, improved access to information and an enhanced capacity to respond to hazardous events and therefore contributes positively to adaptive capacity. Data were obtained from the ELSTAT at NUTS2 level (ELSTAT, 2011).

Gross Domestic Product (GDP)

Per capita GDP was used as a proxy for the economic prosperity of each region (Eklund et al., 2023). Regions with higher GDP are considered less vulnerable as they consider allocating greater financial resources to prevention, fire suppression infrastructure and organizational capacity to respond to a fire event. Per capita GDP (in euros) was obtained from ELSTAT (ELSTAT, 2022).

Table 2: Vulnerability indicators (sensitivity and adaptive capacity) together with their native resolution and data source.

Risk component	Index	Description	Resolution	Source
Vulnerability (Sensitivity)	Flammability	Intrinsic fuel flammability (vegetation-based)	100m	Bacciu et al. (2021)
	Fuel load	Above ground biomass (living woody parts, dead foliage and dead wood) available for combustion	100m	ECMWF Fuel Characteristics v2 (McNorton & Di Giuseppe, 2024); ESA Climate Change Biomass_cci: Global datasets of forest above-ground biomass v3 (Santoro &

https://doi.org/10.5194/egusphere-2026-4656
Preprint. Discussion started: 7 September 2026

				Cartus, 2024)
	Slope	Terrain steepness; rate of elevation change	90m	GLO-90 Copernicus DEM (European Space Agency, 2021)
	Aspect	Orientation of slope; compass direction it faces	90m	GLO-90 Copernicus DEM (European Space Agency, 2021)
	Energy transmission networks	Proximity to overhead power lines (>45kV)	-	Open Street Map (OSM) (OpenStreetMap contributors, 2025)
Vulnerability (Adaptive Capacity)	Firefighters	Permanent and seasonal firefighters and volunteers of the Fire Brigade (people/km^2)	NUTS2	Hellenic Fire Service (authors personal communication)
	GDP	Per Capita Gross Domestic Product (in euro)	NUTS2	Hellenic Statistical Authority (ELSTAT, 2022)
	Educational level	Percentage of the population with tertiary education	NUTS2	Hellenic Statistical Authority (ELSTAT, 2011)
	Occupation in primary sector	People per km^2 working in the primary sector	NUTS2	Hellenic Statistical Authority (ELSTAT, 2020)

2.3 Indicator preprocessing and normalization

As the selected indicators differ in their nature and measurement scale, a series of preprocessing and normalization procedures were applied before aggregation to ensure a consistent interpretation of the wildfire risk components. The adopted procedures depended on the characteristics of each indicator and included binary classification, threshold-based classification and min–max normalization.

Binary indicators, including forest areas, agricultural areas, protected areas and WUI, were retained as binary variables representing the presence or absence of the corresponding feature.

For the slope and aspect indicators, the classification scheme of Papanikolaou et al. (2012) was applied. Slope was categorized into three classes: 0–13% (normalized value of 20), 13.1–40% (60), and >40.1% (100)—while aspect was classified into 0°–45° and 316°–360° (20), 46°–134° (40) and 271°–315° (60), and 135°–270° (100).

For the flammability index, the five-class system of Bacciu et al. (2022) was adopted (1.0–1.8: very low, 1.8–2.6: low, 2.6–3.4: medium, 3.4–4.2: high, >4.2: very high), with each class assigned proportionally to the 0–100 normalized scale (20, 40, 60, 80, 100, respectively). Land cover types considered non-flammable were assigned a value of 0 to reflect the absence of ignition potential.

https://doi.org/10.5194/egusphere-2026-4656
Preprint. Discussion started: 7 September 2026

Finally, concerning the proximity to power transmission networks the classification proposed by the Ministry of the Environment classification (Ministry of Environment and Energy, 2020) was implemented and the respective 0-100 values were assigned as follows: (a) pixels outside the 150 m buffer zone (0), (b) pixels at the buffer zone at elevation <600 m (100), (c) pixels at the buffer zone at elevation 600-1200 m (80), and (d) pixels at the buffer zone at elevation >1200 m (60).

Continuous variables (biomass, GDP, educational level, occupation rate in the primary sector) were normalized to a common scale ranging from 0 to 100 using min–max normalization. This method converts all values to 0-100 scores ranging by subtracting the minimum score, dividing by the range of the indicator values, and multiplying by 100 (GIZ & EURAC, 2017).

Hazard indicators were treated separately. Instead of statistical normalization, FFMC90, ISI90 and FWI90 were classified using the operational thresholds adopted by the European Forest Fire Information System (EFFIS). This approach preserves the operational interpretation of fire danger classes and ensures consistency with the thresholds currently used for wildfire danger assessment across Europe.

Most indicators considered in this study were normalized using min–max scaling because they have either a finite range or meaningful observed limits. However, by applying a min–max transformation to firefighter density (firefighters km^{-2}) would assign the municipality with the highest observed firefighter density a normalized value of one, implicitly treating this municipality as having full adaptive capacity. As the contribution of additional firefighting resources to adaptive capacity is expected to decrease as density increases, firefighter density was transformed using a hyperbolic half-saturation function:

$$AC_i = \frac{x_i}{x_i + k} \tag{1}$$

where x_i is firefighter density and k is the half-saturation constant. Half-saturation functions describe nonlinear responses in which the response increases rapidly at low levels and progressively approaches an asymptote, with k representing the value at which half of the maximum response is reached (Mulder and Hendriks, 2014). As there is no documented value defining k for firefighters density, we chose to use the sample median (0.15 firefighters km^{-2}). This choice assigns the median municipality an adaptive-capacity score of 0.5, providing thus a transparent and readily interpretable reference point for this transformation.

For the adaptive capacity indicators the scale was inverted, with higher values representing lower adaptive capacity and, thus, greater vulnerability. This adjustment ensures consistency across all indicators, aligning higher index values with higher levels of fire risk.

Following preprocessing and normalization, all indicator values were aggregated to the municipal level by calculating the mean value within each municipality. These municipal-level values were subsequently used in the wildfire risk assessment.

2.4 Indicator importance using the Analytic Hierarchy Process (AHP)

The relative importance of the wildfire risk components and indicators was determined using the Analytic Hierarchy Process (AHP), a widely used multi-criteria decision-making (MCDA) method based on pairwise comparisons (Saaty, 1980). By

https://doi.org/10.5194/egusphere-2026-4656
Preprint. Discussion started: 7 September 2026

explicitly incorporating expert judgment into complex decision-making problems, AHP has been extensively applied in climate-related risk and adaptation assessments (de Brito & Evers, 2016), including wildfire risk assessment (e.g., Nuthammachot and Stratoulias, 2021; Abdo et al., 2022; Khan et al., 2026).

Pairwise comparisons were obtained through a structured questionnaire completed by an interdisciplinary panel of ten experts with expertise in wildfire management, forestry, climatology, ecology, environmental science, environmental policy, the Fire Service and Civil Protection. Experts evaluated the relative importance of the wildfire risk components and indicators using Saaty's nine-point scale, where values range from 1 (equal importance) to 9 (extreme importance).

The AHP decision hierarchy used in this study is presented in Table 5. The overall objective (Level 0) was wildfire risk assessment. The first hierarchical level comprised the three main risk components (hazard, exposure and vulnerability), followed by the vulnerability sub-components (sensitivity and adaptive capacity) and the corresponding indicators. Pairwise comparison matrices were analysed using the AHP Online System (AHP-OS; Goepel, 2018), which was used to calculate local and global indicator weights, the Consistency Ratio (CR), and the consensus indicator (S*).

The Consistency Ratio (CR) was calculated to assess the logical consistency of expert judgments following Alonso and Lamata (2006). A CR value below 10% was considered acceptable, ensuring the reliability of the derived weights (Goepel, 2018). Finally, the consensus indicator (S*) was calculated to quantify the overall agreement among experts, ranging from 0% (no consensus) to 100% (complete consensus). The resulting local weights were subsequently used in the aggregation frameworks described in Section 2.5.

2.5 Indicator aggregation and composite risk calculation

Two aggregation frameworks were used to calculate the composite wildfire risk index. The first employed the conventional weighted linear combination (Framework A), while the second was based on the Ordered Weighted Averaging (OWA) operator (Framework B). In both frameworks, the relative importance of the individual indicators was represented by the AHP-derived local weights.

Following the IPCC risk framework, wildfire risk was represented through the three core risk components (hazard, exposure and vulnerability). Therefore, the comparison focused on alternative aggregation approaches applied to these components, while maintaining a common weighting scheme for the underlying indicators (Figure 1). In Framework A, normalized indicator values were first aggregated within each risk component using the corresponding AHP-derived local weights to calculate the hazard, exposure and vulnerability component scores. The final wildfire risk index was subsequently obtained through a weighted linear combination of the three component scores using the corresponding AHP-derived component weights. This approach assumes full compensability among the three risk components, whereby low values in one component can be completely compensated by high values from the others. Framework B followed the same procedure for calculating hazard, exposure and vulnerability component scores. However, instead of combining the three components using a weighted linear combination, the final wildfire risk index was obtained by applying the OWA operator directly to the hazard, exposure and vulnerability component scores.

https://doi.org/10.5194/egusphere-2026-4656
Preprint. Discussion started: 7 September 2026

The OWA operator is a multicriteria aggregation method that enables explicit control over aggregation behaviour while preserving the relative importance assigned to the individual indicators during the calculation of the component scores (Yager, 1988; Malczewski, 2006). Unlike the weighted linear combination, OWA allows the degree of compensation among the three risk components to be adjusted through the orness parameter, which ranges from conjunctive (AND-like) to disjunctive (OR-like) aggregation. Lower orness values favour more conservative solutions by giving greater influence on lower component values, whereas higher orness values increasingly emphasize higher component values (Yager, 1996). By applying the OWA operator at the component level, the conceptual structure of the IPCC risk framework is preserved while alternative representations of the interaction between hazard, exposure and vulnerability are enabled.

To evaluate the influence of aggregation behaviour, four orness levels (0.2, 0.4, 0.6 and 0.8) were examined for each hazard indicator (FWI90, FFMC90 and ISI90). For each configuration, wildfire risk was calculated and evaluated against observed wildfire occurrence using Receiver Operating Characteristic (ROC) analysis (see Sect. 2.6). The same validation procedure was applied to both aggregation frameworks to enable direct comparison of their predictive performance. The configuration with the highest predictive performance was subsequently selected for the final wildfire risk assessment. OWA weights were derived using a standard quantifier-based formulation (Yager, 1996; Xu, 2005), with full details provided in Appendix A. The selected OWA configuration was subsequently applied consistently to the baseline and future climate scenarios.

The final wildfire risk was classified into five categories (low, moderate, high, very high and extreme) using the Jenks natural breaks classification method. Classification thresholds were derived from the complete dataset, including the baseline and all future scenarios and subsequently applied across all study periods to enable direct spatial and temporal comparison of wildfire risk.

https://doi.org/10.5194/egusphere-2026-4656
Preprint. Discussion started: 7 September 2026

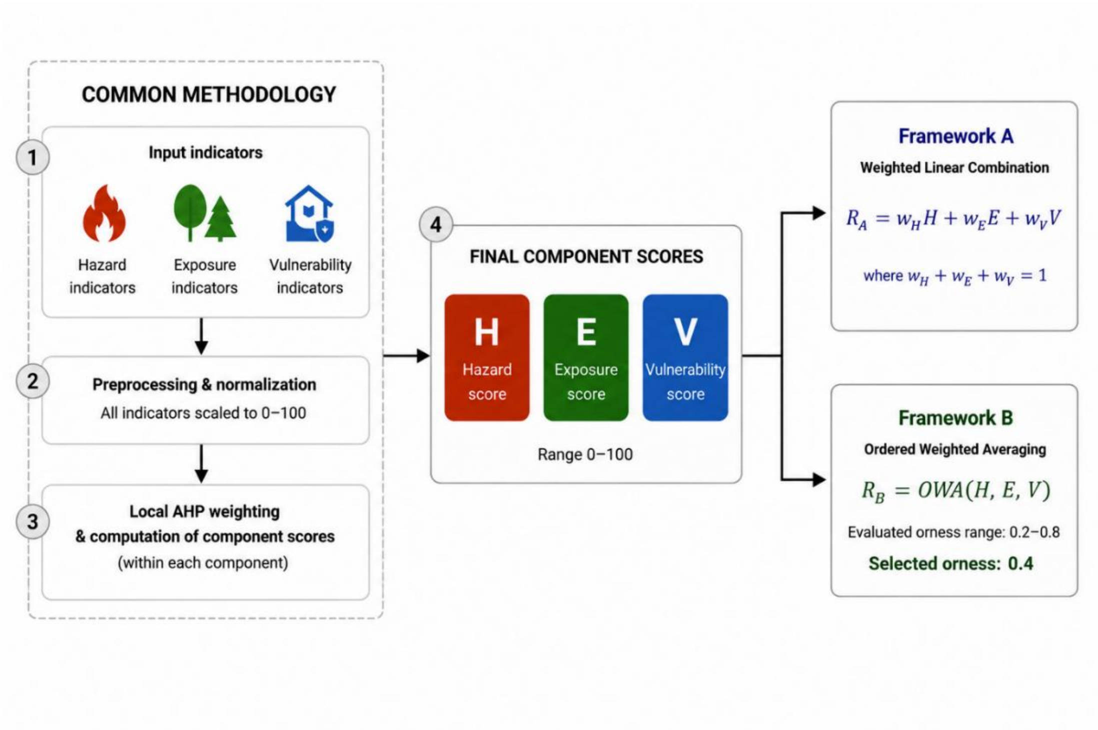

Figure 1: Conceptual workflow of the two aggregation frameworks evaluated in this study.

2.6 Model validation and performance evaluation

The predictive performance of both aggregation frameworks was evaluated using observed wildfire occurrence at the municipal level. Prior to validation, predominantly urban municipalities were masked and excluded from further analysis. Urban municipalities were identified using the Degree of Urbanization (DEGURBA) Level-2 classification derived from the 1-km grid (European Commission, Joint Research Centre and Eurostat, 2011) and were excluded when they were almost entirely composed of dense urban fabric (≥85 % urban core grid cells) and exhibited negligible peri-urban extent (<10 %). The thresholds were selected empirically to exclude predominantly urban municipalities, while retaining those with meaningful peri-urban characteristics relevant to wildfire risk, particularly in the Attica region where municipalities adjacent to the main mountainous areas were intentionally preserved.

Model performance was assessed using Receiver Operating Characteristic (ROC) analysis and the corresponding Area Under the Curve (ROC-AUC), a threshold-independent metric widely used for evaluating continuous susceptibility and risk indices (Fawcett, 2006). Validation was primarily conducted against wildfire occurrence, defined as the presence of at least one recorded wildfire event per municipality during the overlapping period (2000–2014) between the climate baseline and the wildfire records. Historical wildfire occurrence served as an empirical benchmark for evaluating the ability of the alternative methodological frameworks to discriminate between municipalities with and without recorded wildfire occurrence. ROC-

https://doi.org/10.5194/egusphere-2026-4656
Preprint. Discussion started: 7 September 2026

AUC was calculated using a logistic regression model relating the continuous wildfire risk index to the binary wildfire occurrence data.

To assess predictive performance, both 10-fold cross-validation and a stratified 70/30 hold-out validation were performed. Cross-validation provides a robust estimate of out-of-sample model performance across multiple data partitions, whereas the hold-out approach evaluates generalization using an independent stratified test subset (Hastie et al., 2009). In addition, paired bootstrap resampling (5,000 iterations) was performed to assess the robustness of the observed difference in predictive performance between the two aggregation frameworks. Unlike the cross-validation and hold-out analyses described above, the bootstrap analysis was performed using the full validation dataset. For each bootstrap sample, ROC-AUC was recalculated for both frameworks and the difference ($\Delta AUC = AUC_{OWA} - AUC_{linear}$) was computed. The resulting bootstrap distribution was used to estimate the mean ΔAUC and its corresponding 95% confidence interval.

To support the spatial interpretation of model performance, municipalities were further classified according to their agreement with the observed wildfire occurrence benchmark using the optimal threshold derived from the Youden index (Youden, 1950), which identifies the risk threshold that provides the best balance between correctly classifying municipalities with observed wildfire occurrence (sensitivity) and correctly classifying municipalities without wildfire occurrence (specificity). Based on this threshold, each municipality was assigned to one of four diagnostic categories: true positives (TP), true negatives (TN), false positives (FP) and false negatives (FN). These categories describe the spatial agreement between the municipal wildfire risk classification and the historical wildfire occurrence benchmark and were used to facilitate the spatial interpretation of model performance.

2.7 Component contribution analysis and dominant risk drivers

To quantify the relative contribution of hazard, exposure and vulnerability to the composite wildfire risk index, a component contribution analysis was performed at the municipal level. The composite risk index (R) was recalculated iteratively by setting one component to zero at each iteration while preserving the same aggregation framework, AHP-derived local weights and OWA configuration. Component contribution was quantified using the Component Contribution Index (CCI):

$$CCI_i = \frac{R - R_{i=0}}{R} \tag{2}$$

where $R_{i=0}$ is the composite risk obtained after setting the corresponding component score to zero. The CCI value therefore represents the proportional reduction in composite risk associated with the removal of that component's contribution. Due to the non-additive nature of the OWA aggregation, component contributions cannot be linearly decomposed and therefore the resulting CCI values do not necessarily sum to one. To facilitate comparison among components, normalized component contributions (nCCI) were calculated as:

$$nCCI_H = \frac{CCI_H}{CCI_H + CCI_E + CCI_{VUL}} \tag{3}$$

https://doi.org/10.5194/egusphere-2026-4656
Preprint. Discussion started: 7 September 2026

with equivalent formulations for exposure and vulnerability. Municipalities were subsequently classified according to the component with the highest normalized contribution, allowing the identification of the dominant wildfire risk driver.

3 Results

3.1 AHP weighting results

The AHP analysis provided the local weights for wildfire risk components and individual indicators (Table 3). Among the three main components, hazard received the highest weight (35.0%), followed by vulnerability (33.3%) and exposure (31.7%). Within the exposure component, WUI (12.4%) received the highest global weight, followed by forest areas (8.0%) and protected areas (7.4%). Within vulnerability, available biomass (6.2%), flammability (6.1%) and firefighter density (7.8%) emerged as the most influential indicators.

The maximum consistency ratio (CR) of the aggregated pairwise comparison matrices was 2.3%, well below the recommended threshold of 10%, indicating a high level of consistency in the expert judgments. The corresponding group consensus index (S*) reached 71.6%, indicating a satisfactory level of agreement among the participating experts despite their diverse disciplinary backgrounds.

Table 3: Hierarchical structure of the AHP model and corresponding local and global indicator weights.

Level 0	Level 1 Component	Local weight (LW1)	Level 2 sub-component	Local weight (LW2)	Level 3 Indicator	Local weight (LW3)	Global weight (%)
Wildfire risk	Hazard	0.350	-	-	FWI90/ISI90/FFMC90	-	35.00
	Exposure	0.317	-	-	Forest areas	0.252	7.99
			-	-	Agricultural areas	0.125	3.96
			-	-	Protected areas	0.232	7.35
			-	-	WUI	0.391	12.39
	Vulnerability	0.333	Sensitivity	0.508	Flammability	0.361	6.11
					Available biomass	0.366	6.19
					Aspect	0.084	1.42
					Slope	0.090	1.52
					Energy transmission networks	0.098	1.66
			Adaptive	0.492	Firefighters	0.474	7.77

https://doi.org/10.5194/egusphere-2026-4656
Preprint. Discussion started: 7 September 2026

	capacity			
		Educational level	0.087	1.43
		GDP	0.102	1.67
		Occupation in primary sector	0.337	5.52

3.2 Evaluation and selection of the wildfire risk framework

To identify the most appropriate hazard representation and aggregation framework, three fire-weather metrics (FFMC90, ISI90 and FWI90) were evaluated in combination with four OWA orness values (0.2, 0.4, 0.6 and 0.8). Model performance was assessed against observed municipal fire occurrence data using both 10-fold cross-validation (AUC_CV10) and an independent 70/30 hold-out validation (AUC_HO).

Among the evaluated hazard metrics, FFMC90 consistently provided the highest predictive performance across all aggregation settings (Table 4). The best-performing configuration combined FFMC90 with an OWA orness value of 0.4, yielding an AUC_CV10 of 0.729 and an AUC_HO of 0.764, indicating an acceptable ability to distinguish between municipalities that experienced at least one recorded wildfire and those with no recorded wildfire occurrence.

In contrast, FWI90 showed consistently lower predictive performance, with its best configuration obtained at orness = 0.8 (AUC_CV10 = 0.670; AUC_HO = 0.712), while ISI90 exhibited near random predictive performance across all aggregation settings (maximum AUC_CV10 = 0.554; AUC_HO = 0.544). Based on these results, Framework B, combining FFMC90 with an OWA orness value of 0.4, was selected for the subsequent analyses.

To evaluate the effect of the aggregation strategy, Framework B was compared with Framework A, which employed a conventional hierarchical linear weighted aggregation while preserving the same hazard, exposure and vulnerability components and identical AHP-derived weights. Framework B consistently outperformed Framework A, achieving an AUC_CV10 of 0.729 compared with 0.693 for Framework A, while the corresponding hold-out AUC increased from 0.708 to 0.764. These results indicate that OWA aggregation strategy achieved higher predictive performance than the conventional linear aggregation and was therefore selected for the subsequent analyses.

The robustness of the observed improvement in full-sample AUC between the two frameworks was further evaluated using paired bootstrap resampling (5,000 iterations). The estimated difference in full-sample AUC remained positive, with a 95% bias-corrected and accelerated (BCa) confidence interval of 0.001–0.057 ($p = 0.048$), providing statistical support for the observed improvement. Since both frameworks employed the same indicators, hierarchical structure and expert-derived weights, the observed difference can be attributed solely to the aggregation operator. Framework B was therefore adopted as the final structural wildfire risk framework and used in all subsequent analyses, including the assessment of component contributions and future wildfire risk projections.

https://doi.org/10.5194/egusphere-2026-4656
Preprint. Discussion started: 7 September 2026

Table 4: Predictive performance of the evaluated wildfire risk framework configurations using three hazard metrics (FFMC90, FWI90 and ISI90) and four OWA orness values. Model performance was evaluated against observed municipal fire occurrence using 10-fold cross-validation (AUC_CV10) and an independent 70/30 hold-out validation (AUC_HO). The selected configuration used in the subsequent analyses is highlighted in bold.

Hazard	Orness level	AUC_CV10	AUC_HO
FFMC90	0.2	0.696	0.685
	0.4	**0.729**	**0.764**
	0.6	0.650	0.685
	0.8	0.515	0.558
FWI90	0.2	0.606	0.612
	0.4	0.535	0.519
	0.6	0.551	0.563
	0.8	0.670	0.712
ISI90	0.2	0.554	0.544
	0.4	0.521	0.504
	0.6	0.443	0.500
	0.8	0.512	0.537

3.3 Spatial agreement with the historical wildfire occurrence benchmark

To complement the ROC-AUC evaluation, the spatial agreement between the wildfire risk classification and the historical wildfire occurrence benchmark was examined using the optimal Youden threshold (Fig. 2). Of the 304 municipalities included in the validation dataset, 183 (60.2%) were classified as true positives (TP), 35 (11.5%) as true negatives (TN), 34 (11.2%) as false positives (FP) and 52 (17.1%) as false negatives (FN), indicating that approximately 72% of municipalities showed agreement between the wildfire risk classification and the historical wildfire occurrence benchmark.

Figure 2 shows the spatial distribution of municipalities exhibiting agreement (TP and TN) and disagreement (FP and FN) with the historical wildfire occurrence benchmark. True-positive municipalities predominated across much of mainland Greece, whereas false-negative municipalities occurred more frequently in parts of northern and western Greece. False-positive and true-negative municipalities were comparatively fewer and more spatially dispersed. These patterns indicate that the correspondence between wildfire risk classification and historical wildfire occurrence varies geographically, providing additional spatial insight beyond the overall ROC-AUC metric.

https://doi.org/10.5194/egusphere-2026-4656
Preprint. Discussion started: 7 September 2026

Figure 2: Spatial distribution of agreement between municipal wildfire risk classification and observed wildfire occurrence benchmark during the validation period (2000–2014). Municipalities were classified using the optimal national Youden threshold (risk score = 36.69) into true positives (high predicted risk with observed wildfire occurrence), true negatives (low predicted risk without observed wildfire occurrence), false positives (high predicted risk without observed wildfire occurrence), and false negatives (low predicted risk despite observed wildfire occurrence).

3.4 Present-day wildfire risk and dominant risk components

Present-day wildfire risk exhibited substantial spatial variability across Greece (Fig. 3). Municipalities classified as High to Extreme risk were concentrated primarily across western and southern Greece, including large parts of the Peloponnese and Crete, whereas Low and Medium risk classes occurred more frequently in several island municipalities and parts of northern

https://doi.org/10.5194/egusphere-2026-4656
Preprint. Discussion started: 7 September 2026

and central Greece. Based on the global Jenks classification, 15.5% of municipalities were classified as Low risk, 20.7% as Medium, 36.5% as High, 24.0% as Very High and 3.3% as Extreme.

The normalized component contribution maps (Fig. 4) indicate that hazard represented the largest contributor to the composite wildfire risk across most municipalities. Hazard exhibited the highest median normalized contribution (42.2%, IQR: 38.5–46.2%), followed by vulnerability (31.3%, IQR: 27.9–35.1%) and exposure (27.6%, IQR: 24.1–30.7%). Hazard was identified as the dominant component in 83.6% of municipalities, whereas vulnerability and exposure were dominant in 13.5% and 3.0% of municipalities, respectively. Detailed maps of the hazard, exposure and vulnerability component scores used to derive the composite wildfire risk for the current climate are provided in Appendix B.

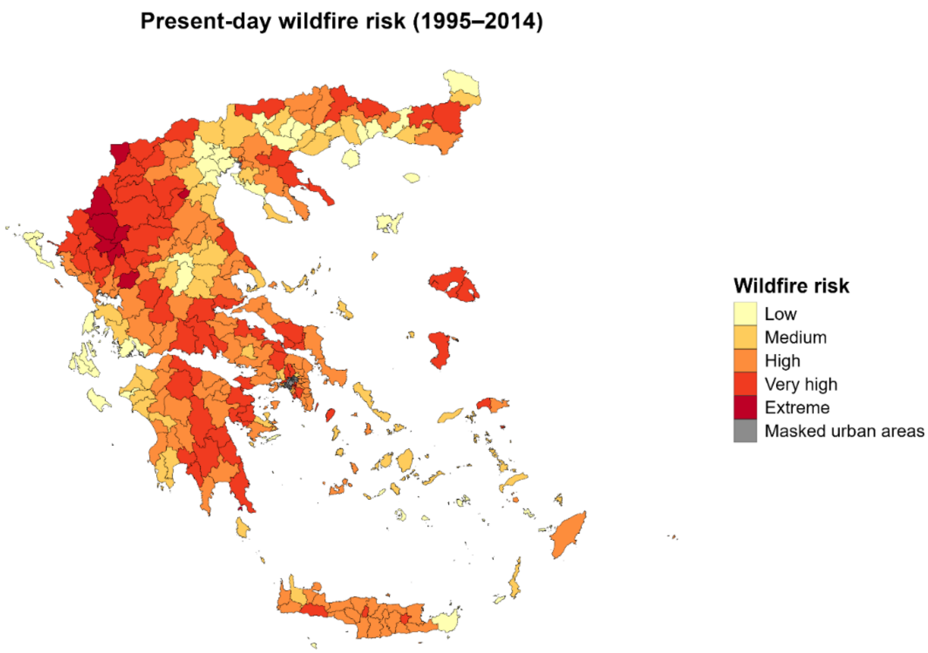

Figure 3: Present-day (1995-2014) wildfire risk across Greek municipalities, classified into five categories using the global Jenks classification.

https://doi.org/10.5194/egusphere-2026-4656
Preprint. Discussion started: 7 September 2026

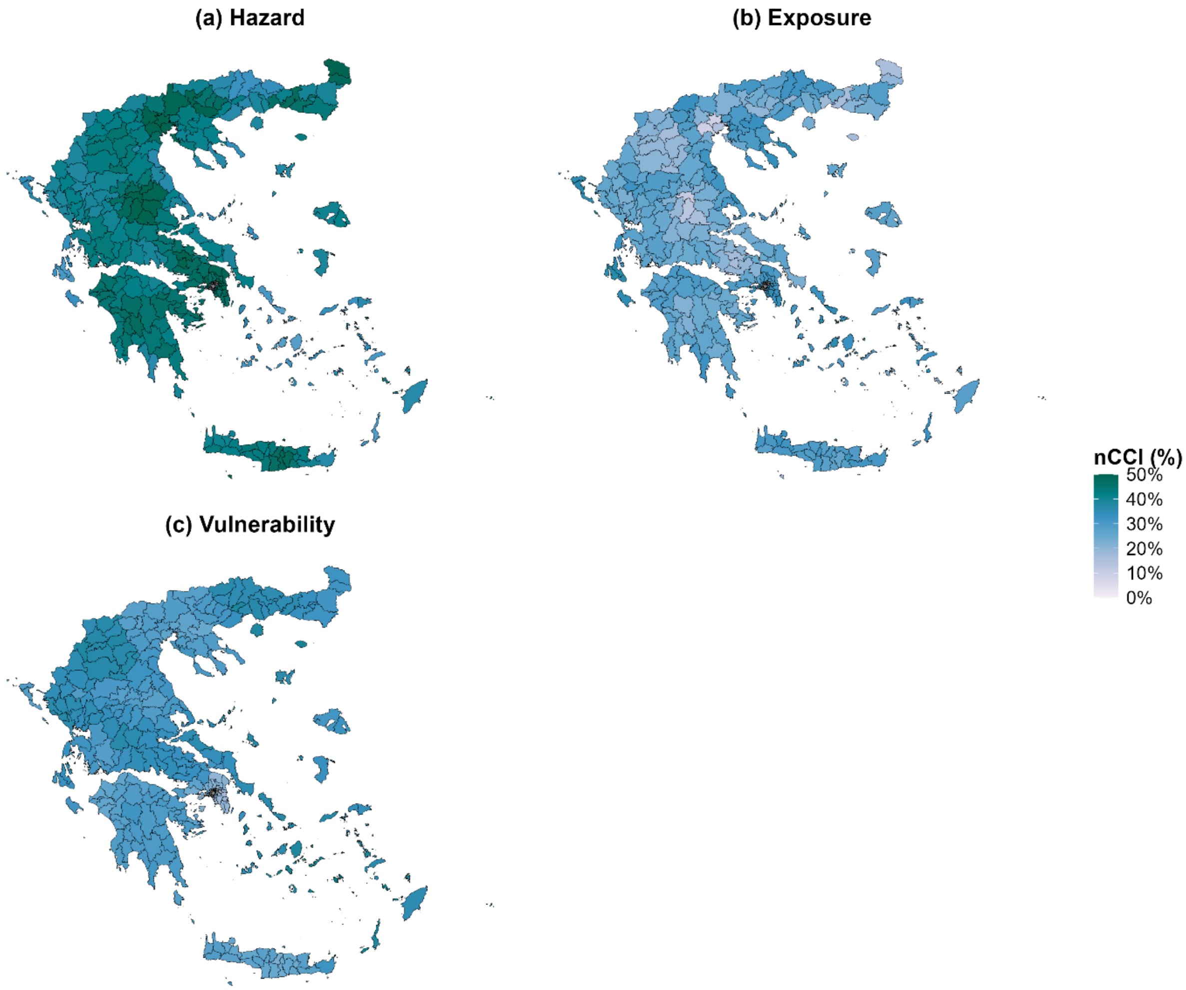

Figure 4: Spatial distribution of the normalized component contributions (nCCI) of hazard, exposure and vulnerability to the present-day wildfire risk.

3.5 Projected shifts in municipal wildfire risk under future climate scenarios

Future climate projections indicate a gradual increase in wildfire risk across Greece under all examined climate scenarios (Fig. 5). The overall spatial pattern of wildfire risk remained broadly consistent, while the magnitude of the increase became progressively larger from the mid-century to the late-century projections and under the high-end SSP5-8.5 scenario. On average, municipal wildfire risk increased by 1.4 and 2.2 risk units in the near future under SSP2-4.5 and SSP5-8.5 scenarios, respectively, reaching 2.1 and 3.7 risk units by the end of the century. Although the increase in the composite risk index was modest, it was consistently observed across the country and resulted in widespread transitions towards higher wildfire risk classes.

Accordingly, the distribution of municipalities shifted progressively towards higher wildfire risk classes under all future climate scenarios (Fig. 6). The proportion of municipalities classified as Very High or Extreme increased from 27.3% during the baseline period to 38.8% under SSP2-4.5 (2041–2060), 45.4% under SSP5-8.5 (2041–2060), 43.7% under SSP2-4.5 (2081–2100), and 56.2% under SSP5-8.5 (2081–2100). This redistribution was accompanied by a decrease in the proportion of municipalities classified as Low and Medium, while the proportion classified as High remained relatively stable before declining in the distant future period under SSP5-8.5 scenario, reflecting a further shift towards the highest wildfire risk categories.

https://doi.org/10.5194/egusphere-2026-4656
Preprint. Discussion started: 7 September 2026

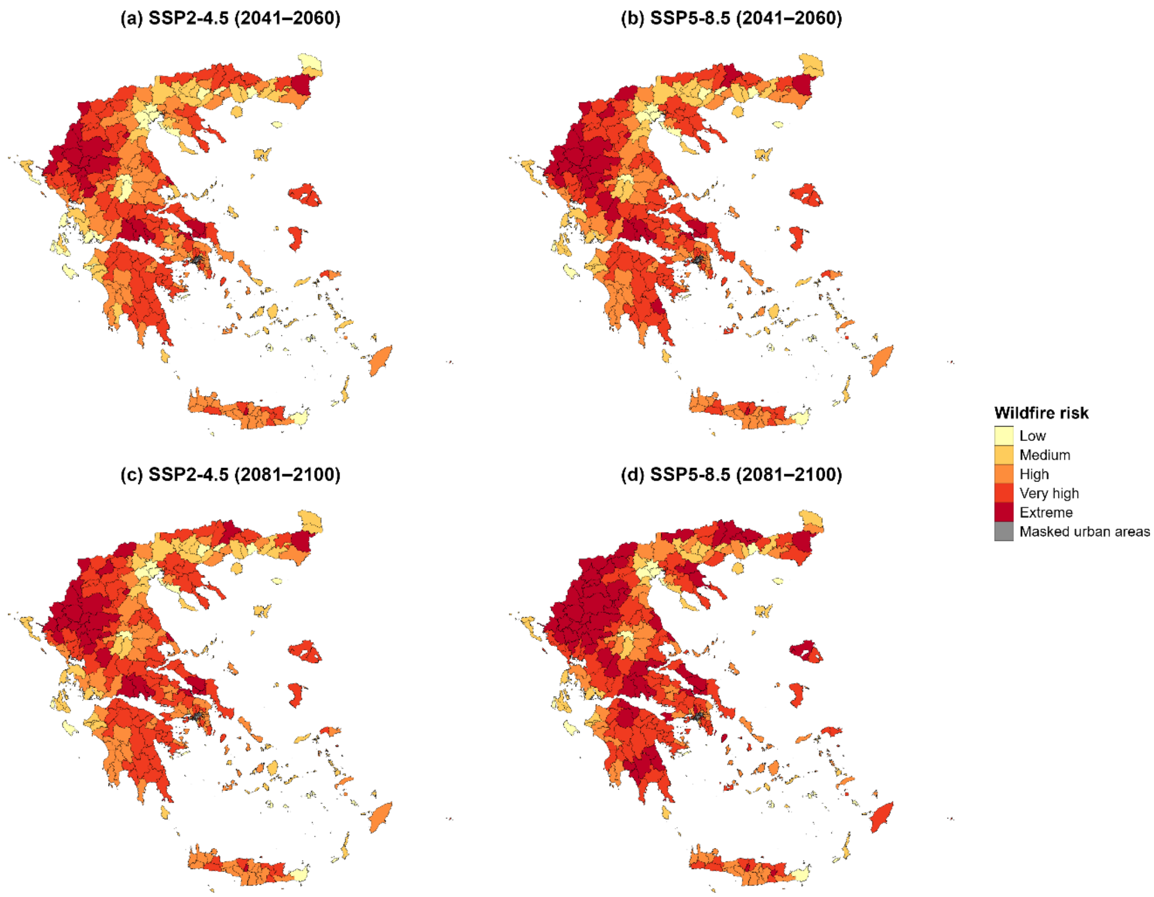

Figure 5: Projected municipal structural wildfire risk under SSP2-4.5 and SSP5-8.5 for the mid-century (2041–2060) and end-of-century (2081–2100) periods. Risk classes were defined using common global Jenks natural breaks derived from the complete dataset to ensure consistent comparison across all future scenarios.

https://doi.org/10.5194/egusphere-2026-4656
Preprint. Discussion started: 7 September 2026

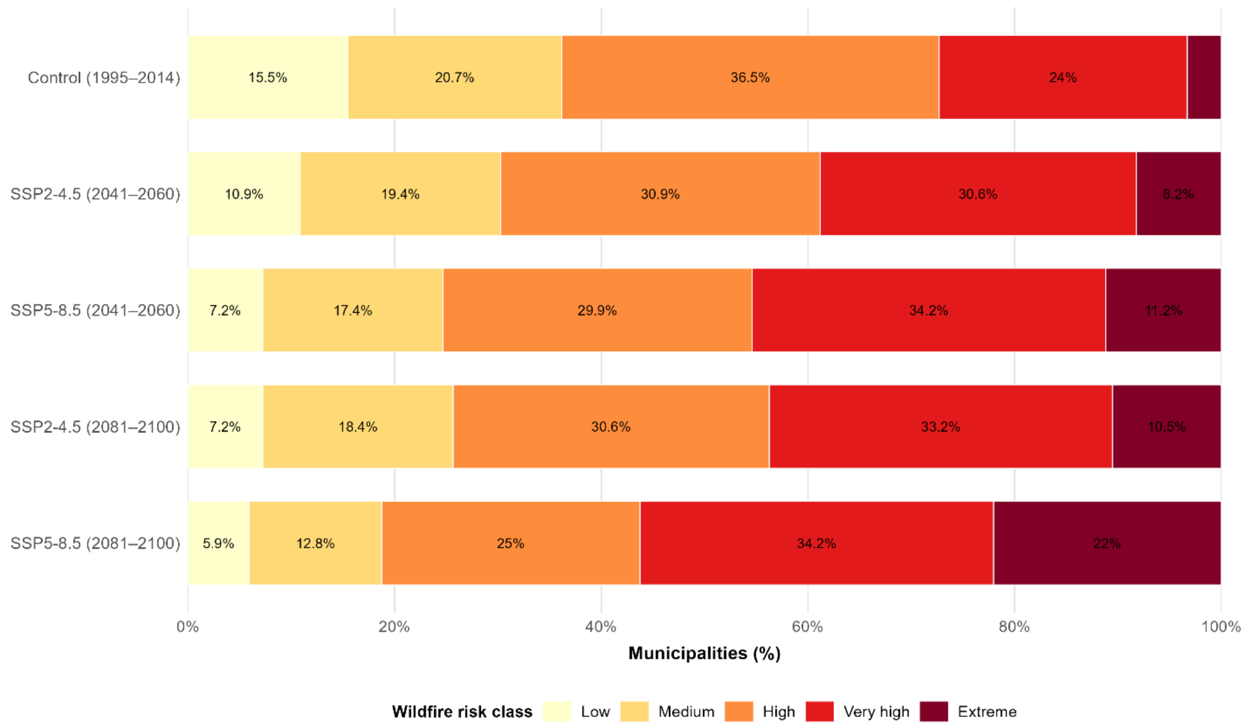

Figure 6: Distribution of Greek municipalities across wildfire risk classes for the reference period (1995–2014) and future climate scenarios.

4. Discussion

4.1 Methodological implications of aggregation method

Our results demonstrate that aggregation method influences the empirical performance of composite wildfire risk indices. Although the two evaluated frameworks incorporated identical hazard, exposure and vulnerability components within the same IPCC risk structure, changing only the aggregation method resulted in measurable differences in their ability to reproduce observed wildfire occurrence. While previous studies have typically applied predefined OWA orness levels to represent alternative decision attitudes (e.g. Özcan et al., 2025; Faramarzi et al., 2021), the present framework evaluated aggregation behaviour as an empirical modelling choice. Different aggregation behaviours were compared against observed wildfire occurrence, allowing the aggregation strategy with the highest predictive performance to be identified while maintaining the same indicators, normalization procedures and weighting scheme. The OWA-based framework achieved a modest but statistically significant improvement over the conventional linear aggregation approach, indicating that the observed performance difference can be attributed to the aggregation operator itself.

https://doi.org/10.5194/egusphere-2026-4656
Preprint. Discussion started: 7 September 2026

The improved performance of the OWA-based framework suggests that aggregation behaviour plays an important role in representing the multidimensional nature of wildfire risk. Compared with fully compensatory linear aggregation, OWA provides greater flexibility in how hazard, exposure and vulnerability interact within the final risk score, highlighting that the aggregation method should be regarded as a substantive modelling choice rather than a technical implementation step in risk calculation. The sensitivity analysis further demonstrated that predictive performance varied across the tested OWA orness values. Within the range of aggregation behaviours evaluated in this study, the highest predictive performance was achieved for an intermediate orness value (0.4), suggesting that a balanced contribution of hazard, exposure and vulnerability provided the most effective representation of wildfire risk.

4.2 Influence of hazard representation on wildfire risk assessment

The comparison of alternative hazard representations (FFMC90, ISI90, FWI90) demonstrated that predictive performance was sensitive to how wildfire hazard was represented within the composite index. Among the three indicators evaluated, FFMC90 consistently showed the highest discriminatory ability with respect to the historical wildfire occurrence benchmark. The stronger performance of FFMC90 is likely related to the physical processes represented by the index. FFMC represents the moisture content of fine dead surface fuels, which respond rapidly to short-term weather conditions and strongly influence ignition probability. Because these fuels are the first to ignite under favourable weather conditions, their moisture status has consistently been identified as a key predictor of fire occurrence in previous studies (Martell et al., 1987; Wotton et al., 2003). This is consistent with the higher predictive performance of FFMC90 observed in the present municipal-scale wildfire risk assessment.

Beyond differences in the physical representation of wildfire hazard, the diagnostic analyses revealed an additional methodological effect. Replacing FFMC90 with FWI90 or ISI90 systematically altered the relative ordering of the hazard, exposure and vulnerability components before aggregation. Under the selected OWA configuration (orness 0.4), FFMC90 ranked as the dominant component in approximately 84% of municipalities, whereas ISI90 most frequently occupied the lowest position. Because OWA assigns positional weights according to rank rather than component identity, changes in H–E–V ordering generated different weighting patterns despite identical aggregation parameters. Consequently, hazard representation influenced not only the information entering the composite index but also the mathematical behaviour of the aggregation process itself.

Overall, the results indicate that predictive performance in rank-based composite wildfire risk indices is governed not only by the physical representation of hazard but also by the interaction between hazard representation and aggregation behaviour. Consequently, these two methodological choices should be considered jointly when interpreting the performance of composite wildfire risk indices.

https://doi.org/10.5194/egusphere-2026-4656
Preprint. Discussion started: 7 September 2026

4.3 Spatial variability and dominant drivers of wildfire risk in Greece

The component contribution analysis demonstrated that hazard was the dominant contributor to composite wildfire risk across most municipalities in Greece. This finding is consistent with the central role of fire weather in shaping wildfire activity in the Mediterranean region (Ruffault et al., 2020). However, the substantial contribution of exposure and vulnerability demonstrates that the spatial distribution of wildfire risk cannot be explained by fire weather alone, but reflects the combined influence of hazard, exposed assets and vulnerability, in accordance with the IPCC risk framework. The observed variability in component contributions indicates that similar levels of composite wildfire risk may arise from different combinations of hazard, exposure and vulnerability. Consequently, municipalities with comparable overall risk may be characterized by different underlying drivers of risk and may therefore require different adaptation priorities. This finding highlights the importance of interpreting the composite risk index together with the contribution of its individual components, particularly when informing adaptation planning.

The spatial distribution of agreement with the historical wildfire occurrence benchmark further indicates that model performance is not spatially uniform across the country. Although agreement was achieved for the majority of municipalities, localized areas of disagreement indicate that the relationship between the wildfire risk classification and historical wildfire occurrence varies geographically. The spatial distribution of disagreement also exhibited geographically coherent patterns, suggesting that regional factors not explicitly represented in the indicator set may influence the correspondence between wildfire risk classification and historical wildfire occurrence. Such variability is expected because historical wildfire occurrence is influenced not only by the underlying wildfire risk, but also by local factors such as ignition patterns and fire suppression effectiveness, which are beyond the scope of the present assessment. These findings reflect the challenges of developing a nationally consistent wildfire risk framework for a country characterized by diverse environmental and socio-economic conditions. The proposed framework prioritizes methodological consistency and comparability across municipalities while providing a transparent basis for identifying broad spatial patterns and the dominant drivers of wildfire risk, thereby supporting adaptation planning at the national scale.

4.4 Implications for climate change adaptation

The proposed framework provides a practical tool for supporting climate change adaptation planning by enabling consistent assessment of wildfire risk under both present and future climatic conditions. By combining projected changes in fire danger with relatively stable exposure and vulnerability characteristics, the framework allows the identification of municipalities where climate change is expected to increase structural wildfire risk, thereby supporting the prioritization of adaptation efforts. This information is particularly relevant for the implementation and revision of Regional Adaptation Action Plans (RAAPs) under the Greek Climate Law (Law 4936/2022), which require spatially explicit climate risk assessments to support the identification and prioritization of adaptation measures. The municipal-scale implementation presented here

https://doi.org/10.5194/egusphere-2026-4656
Preprint. Discussion started: 7 September 2026

provides a consistent and transparent basis for comparing wildfire risk across regions while maintaining compatibility with the IPCC risk framework.

5. Conclusions

This study developed and empirically evaluated an integrated framework for wildfire risk assessment under climate change in Greece, based on the IPCC risk concept, and combining climatic, environmental and socioeconomic indicators within a spatial multi-criteria approach. By integrating expert-derived weighting through the Analytic Hierarchy Process (AHP) with Ordered Weighted Averaging (OWA) aggregation, the proposed methodology enabled a systematic evaluation of how different aggregation behaviours influence the representation and predictive performance of wildfire risk indices.

A central finding of this study is that the performance of composite wildfire risk indices depends not only on indicator selection and weighting, but also critically on the aggregation framework used to combine them. Compared with the conventional fully compensatory linear aggregation, the OWA-based approach provided consistently better agreement with observed wildfire occurrence while preserving the multi-component representation of wildfire risk defined by the IPCC framework. Although hazard emerged as the dominant contributor across most municipalities, exposure and vulnerability remained important components of the final risk assessment, highlighting that wildfire risk cannot be adequately represented by hazard alone.

Beyond its methodological contribution, the proposed framework provides a practical basis for climate change adaptation planning by enabling consistent assessment of current and future wildfire risk at the municipal scale and supporting the prioritization of adaptation actions through spatially explicit information on wildfire risk and its underlying components.

The present study also has several limitations that provide opportunities for future research. Future wildfire risk was assessed assuming constant exposure and vulnerability, with projected changes represented only through the hazard component. Incorporating dynamic exposure and vulnerability scenarios would provide a more comprehensive representation of future wildfire risk. Furthermore, as the methodology was developed and calibrated for Greece, its transferability to other wildfire-prone regions should be evaluated using locally relevant indicators, expert knowledge and empirical validation. Despite these limitations, the proposed framework demonstrates how the IPCC risk concept can be translated into a transparent and empirically validated methodology for wildfire risk assessment. More broadly, the study highlights the importance of complementing expert knowledge with empirical evaluation when developing composite wildfire risk indices capable of supporting climate adaptation in Greece and other wildfire-prone regions under a changing climate.

Appendix A: Derivation of OWA order weights

For m normalized criterion values, the Ordered Weighted Averaging (OWA) operator is defined as:

https://doi.org/10.5194/egusphere-2026-4656
Preprint. Discussion started: 7 September 2026

$$\mathrm{OWA}(x) = \sum_{k=1}^{m} v_k \; x_{(k)}, \tag{A1}$$

where $x_{(k)}$ denotes the k-th largest input value after sorting the criteria in descending order, and v_k denotes the corresponding OWA order weight. Thus, the order weights are assigned to the ranked input values rather than to specific wildfire risk components.

The OWA order weights were derived using the Regular Increasing Monotone (RIM) quantifier proposed by Yager (1996):

$$Q(r) = r^{\beta} \tag{A2}$$

where r is the normalized rank position.

The corresponding OWA order weights for m aggregated criteria are computed as:

$$v_k = Q\left(\frac{k}{m}\right) - Q\left(\frac{k-1}{m}\right), \; k = 1, \ldots, m \tag{A3}$$

The aggregation behaviour is controlled by the degree of orness:

$$\mathrm{orness} = \frac{1}{\beta+1} \tag{A4}$$

For the optimal aggregation behaviour identified through the empirical calibration (orness = 0.4), the corresponding parameter is $\beta = 1.5$. The resulting OWA order weights used for aggregating the three wildfire risk components (hazard, exposure and vulnerability) are presented in Table A1. The order weights are assigned to the ranked values, with, v_1, v_2 and v_3 applied to the largest, second largest, and smallest component values, respectively.

Table A1. OWA order weights used for the aggregation of hazard, exposure and vulnerability at orness = 0.4.

Orness	**v_1**	**v_2**	**v_3**
0.40	0.192	0.352	0.456

Appendix B: Spatial distribution of the wildfire risk components

https://doi.org/10.5194/egusphere-2026-4656
Preprint. Discussion started: 7 September 2026

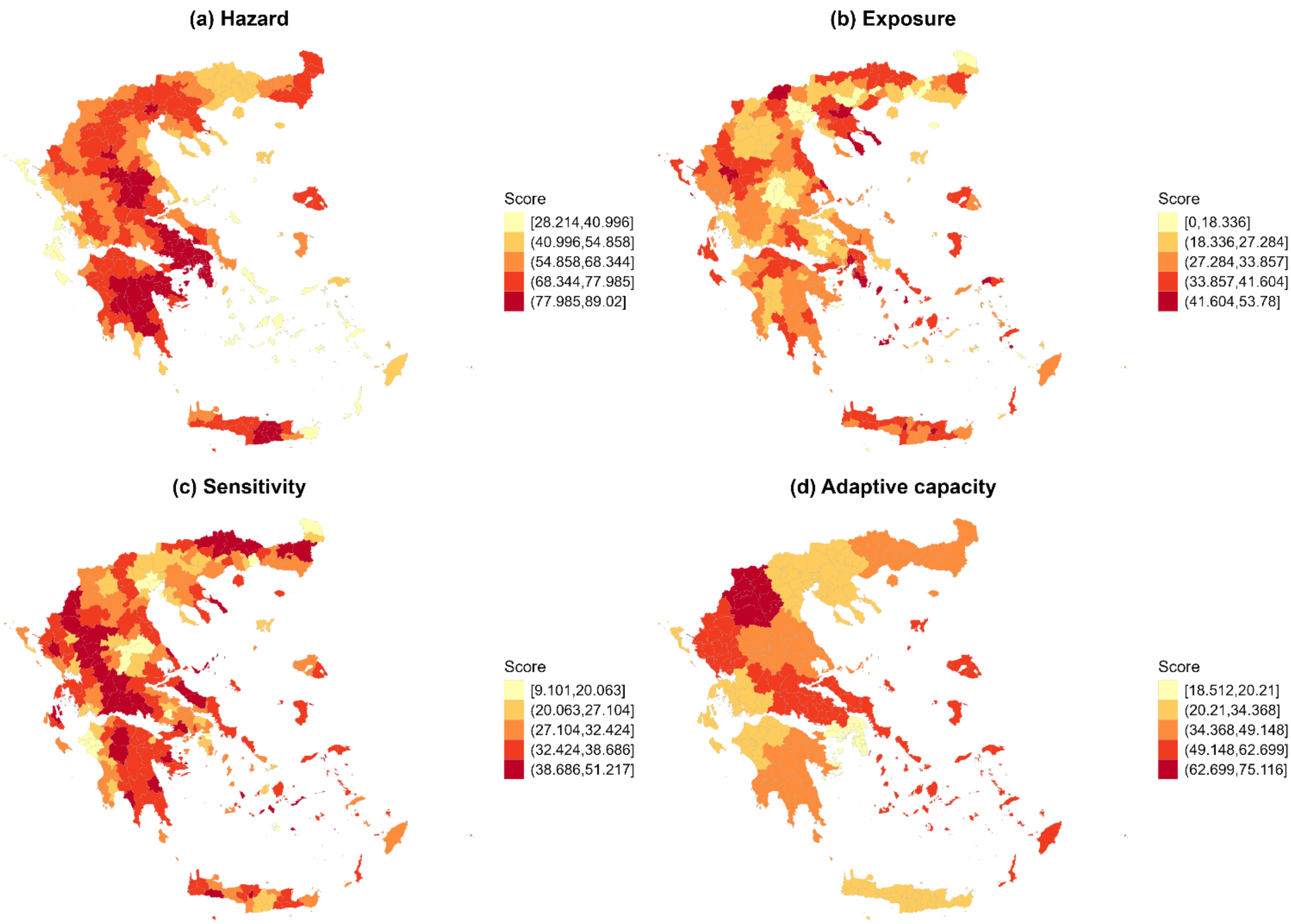

Figure B1. Spatial distribution of the normalized wildfire risk components for the reference period (1995–2014). Sensitivity and adaptive capacity are first aggregated to derive vulnerability. Vulnerability is then combined with hazard and exposure using the Ordered Weighted Averaging (OWA) operator to produce the final composite wildfire risk index.

Data availability

All datasets used in this study are publicly available through the respective online repositories cited in the manuscript, with the exception of the firefighter dataset, which is not publicly available and was obtained from the Hellenic Fire Service. The processed datasets and municipal-scale wildfire risk indicators produced in this study are available from the corresponding author upon reasonable request.

Author contributions

AKa conceptualized the study, developed the methodology and software, performed the formal analysis, validation and visualization, curated the data, and wrote the original draft of the manuscript. KVV and AKo contributed to the formal analysis and data curation. VA contributed to the formal analysis. NF contributed to data curation and reviewed the manuscript. CG supervised the study, acquired funding, and provided resources. MH conceptualized the study, supervised the research, and reviewed the manuscript. All authors read and approved the final manuscript.

Competing interests

The authors declare that they have no conflict of interest.

Acknowledgements

The authors gratefully acknowledge the valuable contributions of the expert panel involved in the selection and weighting of the wildfire risk indicators. Their expertise was essential for the development of the expert-based weighting scheme.

Financial support

This research has received funding from the project "Projecting the impacts of climate change on forest ecosystems in Greece - An integrated forest vulnerability and mitigation framework", which is implemented by the University of the Aegean and funded by the Green Fund, Funding Programme: 'Natural Environment and Innovative Actions 2023'. Priority Axis 3: 'Research and Implementation'.

References

Abdo, H. G., Almohamad, H., Al Dughairi, A. A., and Al-Mutiry, M.: GIS-Based Frequency Ratio and Analytic Hierarchy Process for Forest Fire Susceptibility Mapping in the Western Region of Syria, Sustainability, 14, 4668, https://doi.org/10.3390/su14084668, 2022.

Alonso, J. A. and Lamata, M. T.: Consistency in the analytic hierarchy process: a new approach, Int. J. Unc. Fuzz. Knowl. Based Syst., 14, 445–459, https://doi.org/10.1142/S0218488506004114, 2006.

Bacciu, V., Hatzaki, M., Karali, A., Cauchy, A., Giannakopoulos, C., Spano, D., and Briche, E.: Investigating the Climate-Related Risk of Forest Fires for Mediterranean Islands' Blue Economy, Sustainability, 13, 10004, https://doi.org/10.3390/su131810004, 2021.

Bedia, J., Herrera, S., Camia, A., Moreno, J. M., and Gutiérrez, J. M.: Forest fire danger projections in the Mediterranean using ENSEMBLES regional climate change scenarios, Clim. Change, 122, 185–199, https://doi.org/10.1007/s10584-013-1005-z, 2014.

Carnicer, J., Alegria, A., Giannakopoulos, C., Di Giuseppe, F., Karali, A., Koutsias, N., Lionello, P., Parrington, M., and Vitolo, C.: Global warming is shifting the relationships between fire weather and realized fire-induced CO2 emissions in Europe, Sci Rep, 12, 10365, https://doi.org/10.1038/s41598-022-14480-8, 2022.

Chuvieco, E., Yebra, M., Martino, S., Thonicke, K., Gómez-Giménez, M., San-Miguel, J., Oom, D., Velea, R., Mouillot, F., Molina, J. R., et al.: Towards an integrated approach to wildfire risk assessment: When, where, what and how may the landscapes burn, *Fire*, **6**, 215, https://doi.org/10.3390/fire6050215, 2023.

Colantoni, A., Egidi, G., Quaranta, G., D'Alessandro, R., Vinci, S., Turco, R., and Salvati, L.: Sustainable Land Management, Wildfire Risk and the Role of Grazing in Mediterranean Urban-Rural Interfaces: A Regional Approach from Greece, Land, 9, 21, https://doi.org/10.3390/land9010021, 2020.

Copernicus Land Monitoring Service (CLMS): Corine Land Cover (CLC) 2018 [data set], version 2020_20u1, European Environment Agency (EEA), https://doi.org/10.2909/960998c1-1870-4e82-8051-6485205ebbac, last access: 29 July 2026, 2020.

Copernicus Climate Change Service (C3S): CMIP6 climate projections [data set], Copernicus Climate Change Service (C3S) Climate Data Store (CDS), version 1, https://doi.org/10.24381/cds.c866074c, last access: 29 July 2026, 2021.

de Brito, M. M. and Evers, M.: Multi-criteria decision-making for flood risk management: a survey of the current state of the art, Natural Hazards and Earth System Sciences, 16, 1019–1033, https://doi.org/10.5194/nhess-16-1019-2016, 2016.

Döscher, R., Acosta, M., Alessandri, A., Anthoni, P., Arsouze, T., Bergman, T., Bernardello, R., Boussetta, S., Caron, L.-P., Carver, G., et al.: The EC-Earth3 Earth system model for the Coupled Model Intercomparison Project 6, Geosci. Model Dev., 15, 2973–3020, https://doi.org/10.5194/gmd-15-2973-2022, 2022.

Dupuy, J.-L., Fargeon, H., Martin-StPaul, N., Pimont, F., Ruffault, J., Guijarro, M., Hernando, C., Madrigal, J., and Fernandes, P.: Climate change impact on future wildfire danger and activity in southern Europe: A review, Ann. For. Sci., 77, 35, https://doi.org/10.1007/s13595-020-00933-5, 2020.

Eklund, G., Sibilia, A., Salvi, A., Antofie, T.-E., Rodomonti, D., Salari, S., Poljansek, K., Marzi, S., Gyenes, Z., and Corbane, C.: Towards a European-wide vulnerability framework, Publications Office of the European Union, Luxembourg, https://doi.org/10.2760/353889, 2023.

El Garroussi, S., Di Giuseppe, F., Barnard, C., and Wetterhall, F.: Europe faces up to tenfold increase in extreme fires in a warming climate, npj Clim Atmos Sci, 7, 1–11, https://doi.org/10.1038/s41612-024-00575-8, 2024.

El Mazi, M., Boutallaka, M., Saber, E., Chanyour, Y., and Bouhlal, A.: Forest fire risk modeling in Mediterranean forests using GIS and AHP method: case of the high Rif forest massif (Morocco), Euro-Mediterr J Environ Integr, 9, 1109–1123, https://doi.org/10.1007/s41207-024-00591-3, 2024.

Hastie, T., Tibshirani, R., and Friedman, J.: Model Assessment and Selection, in: The Elements of Statistical Learning: Data Mining, Inference, and Prediction, edited by: Hastie, T., Tibshirani, R., and Friedman, J., Springer, New York, NY, 219–259, https://doi.org/10.1007/978-0-387-84858-7_7, 2009.

Hellenic Statistical Authority (ELSTAT): Population and Housing Census 2011: Resident population by educational attainment [in Greek], available at: https://www.statistics.gr/el/statistics/-/publication/SAM03/2011, last access: 29 July 2026, 2011.

Hellenic Statistical Authority (ELSTAT): Employment in agriculture, 2020, available at: https://www.statistics.gr/en/statistics/-/publication/SPG11/-, last access: 29 July 2026, 2020.

Hellenic Statistical Authority (ELSTAT): Regional accounts: Gross domestic product, 2022, available at: https://www.statistics.gr/en/statistics/-/publication/SEL48/2022 , last access: 29 July 2026, 2022.

European Commission, Joint Research Centre (JRC), and Eurostat: Degree of Urbanisation (DEGURBA) – Level 2, 1 km grid, reference year 2011 [data set], available at: https://ec.europa.eu/eurostat/web/gisco/geodata/population-distribution/degree-urbanisation, last access: 29 July 2026, 2011.

European Space Agency (ESA): Copernicus Digital Elevation Model (Copernicus DEM) GLO-90 [data set], https://doi.org/10.5270/ESA-c5d3d65, 2021.

Faramarzi, H., Hosseini, S. M., Pourghasemi, H. R., and Farnaghi, M.: Forest fire spatial modelling using ordered weighted averaging multi-criteria evaluation, Journal of Forest Science, 67, 87–100, https://doi.org/10.17221/50/2020-JFS, 2021.

Fawcett, T.: An introduction to ROC analysis, Pattern Recognition Letters, 27, 861–874, https://doi.org/10.1016/j.patrec.2005.10.010, 2006.

Georgoulias, A. K., Akritidis, D., Kalisoras, A., Kapsomenakis, J., Melas, D., Zerefos, C. S., and Zanis, P.: Climate change projections for Greece in the 21st century from high-resolution EURO-CORDEX RCM simulations, Atmospheric Research, 271, 106049, https://doi.org/10.1016/j.atmosres.2022.106049, 2022.

GIZ and EURAC: Risk supplement to the Vulnerability Sourcebook: Guidance on how to apply the Vulnerability Sourcebook's approach with the new IPCC AR5 concept of climate risk, GIZ, Bonn, Germany, 2017.

Goepel, K. D.: Implementation of an Online Software Tool for the Analytic Hierarchy Process (AHP-OS), International Journal of the Analytic Hierarchy Process, 10, https://doi.org/10.13033/ijahp.v10i3.590, 2018.

Grünig, M., Seidl, R., and Senf, C.: Increasing aridity causes larger and more severe forest fires across Europe, Glob. Change Biol., 29, 1648–1659, https://doi.org/10.1111/gcb.16547, 2023.

IPCC: Climate Change 2014: Impacts, Adaptation, and Vulnerability. Part A: Global and Sectoral Aspects. Contribution of Working Group II to the Fifth Assessment Report of the Intergovernmental Panel on Climate Change, edited by: Field, C. B., Barros, V. R., Dokken, D. J., Mach, K. J., Mastrandrea, M. D., Bilir, T. E., Chatterjee, M., Ebi, K. L., Estrada, Y. O., Genova, R. C., et al., Cambridge University Press, Cambridge, UK and New York, NY, USA, 2014.

IPCC: Climate Change 2022: Impacts, Adaptation and Vulnerability. Contribution of Working Group II to the Sixth Assessment Report of the Intergovernmental Panel on Climate Change, edited by: Pörtner, H.-O., Roberts, D. C., Tignor, M., Poloczanska, E. S., Mintenbeck, K., Alegría, A., Craig, M., Langsdorf, S., Löschke, S., Möller, V., Okem, A., and Rama, B., Cambridge University Press, Cambridge, UK and New York, NY, USA, https://doi.org/10.1017/9781009325844, 2022.

Karali, A., Varotsos, K. V., Giannakopoulos, C., Nastos, P. P., and Hatzaki, M.: Seasonal fire danger forecasts for supporting fire prevention management in an eastern Mediterranean environment: the case of Attica, Greece, Nat. Hazards Earth Syst. Sci., 23, 429–445, https://doi.org/10.5194/nhess-23-429-2023 , 2023.

Khan, M. A., Gupta, A., Sharma, P., and Roy, A.: Investigation of wildfire risk and its mapping using GIS-integrated AHP method: A case study over Hoshangabad Forest Division in central India, Environ. Dev. Sustain., 28, 8681–8715, https://doi.org/10.1007/s10668-024-05225-w, 2026.

Lamat, R., Kumar, M., Kundu, A., and Lal, D.: Forest fire risk mapping using analytical hierarchy process (AHP) and earth observation datasets: a case study in the mountainous terrain of Northeast India, SN Appl. Sci., 3, 425, https://doi.org/10.1007/s42452-021-04391-0, 2021.

Malczewski, J.: Ordered weighted averaging with fuzzy quantifiers: GIS-based multicriteria evaluation for land-use suitability analysis, International Journal of Applied Earth Observation and Geoinformation, 8, 270–277, https://doi.org/10.1016/j.jag.2006.01.003, 2006.

Marquez Torres, A., Signorello, G., Kumar, S., Adamo, G., Villa, F., and Balbi, S.: Fire risk modeling: an integrated and data-driven approach applied to Sicily, Natural Hazards and Earth System Sciences, 23, 2937–2959, https://doi.org/10.5194/nhess-23-2937-2023, 2023.

Martell, D. L., Otukol, S., and Stocks, B. J.: A logistic model for predicting daily people-caused forest fire occurrence in Ontario, Can. J. For. Res., 17, 394–401, https://doi.org/10.1139/x87-068, 1987.

McNorton, J. R. and Di Giuseppe, F.: A global fuel characteristic model and dataset for wildfire prediction, Biogeosciences, 21, 279–300, https://doi.org/10.5194/bg-21-279-2024, 2024.

Ministry of Environment and Energy: National Strategy for Forests 2018–2038 [in Greek], available at: https://faolex.fao.org/docs/pdf/gre187348.pdf , last access: 29 July 2026), 2018.

Ministry of Environment and Energy: Update of technical specifications for drafting Forest Fire Protection Plans (Ministerial Decision ΥΠΕΝ/ΔΠΔ/61247/2789/26-06-2020) [in Greek], available at: https://dasarxeio.com/wp-content/uploads/2020/07/61247_2789_2020.pdf, last access: 19 June 2025, 2020.

Mouillot, F., Ratte, J.-P., Joffre, R., Moreno, J. M., and Rambal, S.: Some determinants of the spatio-temporal fire cycle in a mediterranean landscape (Corsica, France), Landscape Ecol, 18, 665–674, https://doi.org/10.1023/B:LAND.0000004182.22525.a9, 2003.

https://doi.org/10.5194/egusphere-2026-4656
Preprint. Discussion started: 7 September 2026

Mulder, C. and Hendriks, A. J.: Half-saturation constants in functional responses, Global Ecology and Conservation, 2, 161–169, https://doi.org/10.1016/j.gecco.2014.09.006, 2014.

Müller, W. A., Jungclaus, J. H., Mauritsen, T., Baehr, J., Bittner, M., Budich, R., Bunzel, F., Esch, M., Ghosh, R., Haak, H., Ilyina, T., Kleine, T., Kornblueh, L., Li, H., Modali, K., Notz, D., Pohlmann, H., Roeckner, E., Stemmler, I., Tian, F., and Marotzke, J.: A Higher-resolution Version of the Max Planck Institute Earth System Model (MPI-ESM1.2-HR), Journal of Advances in Modeling Earth Systems, 10, 1383–1413, https://doi.org/10.1029/2017MS001217, 2018.

Muñoz Sabater, J.: ERA5-Land hourly data from 1950 to present [data set], Copernicus Climate Change Service (C3S) Climate Data Store (CDS), https://doi.org/10.24381/cds.e2161bac, last access: 19 June 2025, 2019.

Muñoz-Sabater, J., Dutra, E., Agustí-Panareda, A., Albergel, C., Arduini, G., Balsamo, G., Boussetta, S., Choulga, M., Harrigan, S., Hersbach, H., Martens, B., Miralles, D. G., Piles, M., Rodríguez-Fernández, N. J., Zsoter, E., Buontempo, C., and Thépaut, J.-N.: ERA5-Land: A state-of-the-art global reanalysis dataset for land applications, Earth Syst. Sci. Data, 13, 4349–4383, https://doi.org/10.5194/essd-13-4349-2021, 2021.

Nuthammachot, N. and Stratoulias, D.: Multi-criteria decision analysis for forest fire risk assessment by coupling AHP and GIS: Method and case study, Environ. Dev. Sustain., 23, 17443–17458, https://doi.org/10.1007/s10668-021-01394-0, 2021.

OECD: Taming Wildfires in the Context of Climate Change, OECD Publishing, Paris, https://doi.org/10.1787/dd00c367-en, 2023.

OECD: Taming Wildfires in the Context of Climate Change: The Case of Greece, OECD Environment Policy Papers, No. 43, OECD Publishing, Paris, https://doi.org/10.1787/cfb797a7-en, 2024.

Oom, D., de Rigo, D., Pfeiffer, H., Branco, A., Ferrari, D., Grecchi, R., Artés-Vivancos, T., Houston Durrant, T., Boca, R., Maianti, P., Libertá, G., San-Miguel-Ayanz, J., et al.: Pan-European wildfire risk assessment, EUR 31160 EN, Publications Office of the European Union, Luxembourg, https://doi.org/10.2760/9429, 2022.

Oliveira, S., Moreira, F., Boca, R., San-Miguel-Ayanz, J., and Pereira, J. M. C.: Assessment of fire selectivity in relation to land cover and topography: A comparison between southern European countries, Int. J. Wildland Fire, **23**, 620–630, https://doi.org/10.1071/WF12053, 2014.

OpenStreetMap contributors: OpenStreetMap [power line data], available at: https://www.openstreetmap.org, last access: 19 June 2025, 2025.

Özcan, Z., Caglayan, İ., Kabak, Ö., and Kılıç Gül, F.: Integrated risk mapping for forest fire management using the analytical hierarchy process and ordered weighted average: a case study in southern Turkey, Nat Hazards, 121, 959–1001, https://doi.org/10.1007/s11069-024-06810-y, 2025.

Papanikolaou, D., Papanikolaou, I., and Deligiannakis, G.: Training Material – Guide for Drafting a Forest Fire Prevention Action Plan, Laboratory of Prevention and Management of Natural Disasters, National and Kapodistrian University of Athens, ForestLife–Cities LIFE+ Project, Athens, Greece, 2012.

Robinne, F.-N., Burns, J., Kant, P., de Groot, B., Flannigan, M. D., Kleine, M., and Wotton, B. M. (Eds.): Global fire challenges in a warming world, IUFRO Occasional Paper No. 32, International Union of Forest Research Organizations (IUFRO), Vienna, Austria, 2018.

Rothermel, R. C.: A mathematical model for predicting fire spread in wildland fuels, Research Paper INT-115, Intermountain Forest and Range Experiment Station, U.S. Department of Agriculture, Forest Service, Ogden, UT, USA, 40 pp., 1972.

Rovithakis, A., Grillakis, M. G., Seiradakis, K. D., Giannakopoulos, C., Karali, A., Field, R., Lazaridis, M., and Voulgarakis, A.: Future climate change impact on wildfire danger over the Mediterranean: the case of Greece, Environ. Res. Lett., 17, 045022, https://doi.org/10.1088/1748-9326/ac5f94, 2022.

Ruffault, J., Curt, T., Moron, V., Trigo, R. M., Mouillot, F., Koutsias, N., Pimont, F., Martin-StPaul, N., Barbero, R., Dupuy, J.-L., Russo, A., and Belhadj-Khedher, C.: Increased likelihood of heat-induced large wildfires in the Mediterranean Basin, Sci. Rep., 10, 13790, https://doi.org/10.1038/s41598-020-70069-z, 2020.

Saaty, T. L.: What is the Analytic Hierarchy Process?, in: Mathematical Models for Decision Support, 109–121, https://doi.org/10.1007/978-3-642-83555-1_5, 1988.

Santoro, M. and Cartus, O.: ESA Biomass Climate Change Initiative (Biomass_cci): Global datasets of forest above-ground biomass for the years 2010, 2015, 2016, 2017, 2018, 2019, 2020 and 2021, version 5.01 [data set], NERC EDS Centre for Environmental Data Analysis, https://doi.org/10.5285/bf535053562141c6bb7ad831f5998d77, 2024.

Schug, F., Bar-Massada, A., Carlson, A. R., Cox, H., Hawbaker, T. J., Helmers, D., Hostert, P., Kaim, D., Kasraee, N. K., Martinuzzi, S., Mockrin, M. H., Pfoch, K. A., and Radeloff, V. C.: Map of the global wildland-urban interface [data set], Zenodo, https://doi.org/10.5281/zenodo.7941460, last access: 29 July 2026, 2023.

Stocks, B. J., Lawson, B. D., Alexander, M. E., Van Wagner, C. E., McAlpine, R. S., Lynham, T. J., and Dubé, D. E.: The Canadian Forest Fire Danger Rating System: An overview, For. Chron., 65, 450–457, https://doi.org/10.5558/tfc65450-6, 1989.

Turco, M., Llasat, M. C., Tudela, A., Castro, X., and Provenzale, A.: Brief communication: Decreasing fires in a Mediterranean region (1970–2010, NE Spain), Nat. Hazards Earth Syst. Sci., **13**, 649–652, https://doi.org/10.5194/nhess-13-649-2013, 2013.

Tatebe, H., Ogura, T., Nitta, T., Komuro, Y., Ogochi, K., Takemura, T., Sudo, K., Sekiguchi, M., Abe, M., Saito, F., Chikira, M., Watanabe, S., Mori, M., Hirota, N., Kawatani, Y., Mochizuki, T., Yoshimura, K., Takata, K., O'ishi, R., Yamazaki, D., Suzuki, T., Kurogi, M., Kataoka, T., Watanabe, M., and Kimoto, M.: Description and basic evaluation of simulated mean state, internal variability, and climate sensitivity in MIROC6, Geoscientific Model Development, 12, 2727–2765, https://doi.org/10.5194/gmd-12-2727-2019, 2019.

UNEP-WCMC and IUCN: Protected Planet: The World Database on Protected Areas (WDPA) [data set], June 2025, UNEP World Conservation Monitoring Centre (UNEP-WCMC) and International Union for Conservation of Nature (IUCN), Cambridge, UK, available at: https://www.protectedplanet.net, last access: 29 July 2026, 2025.

https://doi.org/10.5194/egusphere-2026-4656
Preprint. Discussion started: 7 September 2026

van Wagner, C. E.: Development and structure of a Canadian forest fire weather index system, Forestry Technical Report 35, Canadian Forestry Service, Ottawa, Canada, 1987.

Varela, V., Sfetsos, A., Vlachogiannis, D., and Gounaris, N.: Fire Weather Index (FWI) classification for fire danger assessment applied in Greece, Tethys, 15, 31–40, available at: https://www.tethys.cat/en/article/fire-weather-index-fwi-classification-fire-danger-assessment-applied-greece , last access: 29 July 2026), 2018.

Varotsos, K. V., Dandou, A., Papangelis, G., Roukounakis, N., Kitsara, G., Tombrou, M., and Giannakopoulos, C.: Using a new local high resolution daily gridded dataset for Attica to statistically downscale climate projections, Clim Dyn, 60, 2931–2956, https://doi.org/10.1007/s00382-022-06482-z, 2023.

Vilar, L., Gómez, I., Martínez-Vega, J., Echavarría, P., Riaño, D., and Martín, M. P.: Multitemporal modelling of socio-economic wildfire drivers in central Spain between the 1980s and the 2000s: Comparing generalized linear models to machine learning algorithms, PLoS ONE, 11, e0161344, https://doi.org/10.1371/journal.pone.0161344, 2016.

Wotton, B. M., Martell, D. L., and Logan, K. A.: Climate Change and People-Caused Forest Fire Occurrence in Ontario, Climatic Change, 60, 275–295, https://doi.org/10.1023/A:1026075919710, 2003.

Wotton, B. M.: Interpreting and using outputs from the Canadian Forest Fire Danger Rating System in research applications, Environ. Ecol. Stat., 16, 107–131, https://doi.org/10.1007/s10651-007-0084-2 , 2009.

Xanthopoulos, G., Calfapietra, C., and Fernandes, P.: Fire hazard and flammability of European forest types, in: Post-Fire Management and Restoration of Southern European Forests, edited by: Moreira, F., Arianoutsou, M., Corona, P., and De las Heras, J., Springer Netherlands, Dordrecht, the Netherlands, 79–92, https://doi.org/10.1007/978-94-007-2208-8_4, 2012.

Xu, Z.: An overview of methods for determining OWA weights, Int. J. Intell. Syst., 20, 843–865, https://doi.org/10.1002/int.20097, 2005.

Yager, R. R.: On ordered weighted averaging aggregation operators in multicriteria decision making, IEEE Trans. Syst. Man Cybern., 18, 183–190, https://doi.org/10.1109/21.87068, 1988.

Yager, R.R.: Quantifier guided aggregation using OWA operators. Int. J. Intell. Syst., 11, 49-73. https://doi.org/10.1002/(SICI)1098-111X(199601)11:1<49::AID-INT3>3.0.CO;2-Z, 1996.

Youden, W.J.: Index for rating diagnostic tests. Cancer, 3: 32-35. https://doi.org/10.1002/1097-0142(1950)3:1<32::AID-CNCR2820030106>3.0.CO;2-3, 1950